Mathematical Analysis of Omnidirectional Wireless Power Transfer—Part-I: Two-Dimensional Systems

Deyan Lin, *Member, IEEE*, Cheng Zhang, *Student Member, IEEE*, and S. Y. Ron Hui, *Fellow, IEEE*

***Abstract*—This two-part paper aims at providing the basic mathematical theory of omnidirectional wireless power transfer (WPT). Based on current vector control, the magnetic field vector can be generated and pointed at any direction, thus achieving genuine omnidirectional wireless power flow. Part-I of this paper contains the mathematical analysis of the two-dimensional (2-D) system. The 2-D analysis shows that the total input power and the system energy efficiency of the WPT system can be expressed as functions of the angle of the input magnetic field vector. These functions follow the Lemniscates of Bernoulli on the 2-D plane. The directional nature of such curves provides the crucial information of the locations of the receivers so that the wireless power can theoretically be directed to the loads efficiently. The 2-D theory is presented here with the support of experimental verification. Understanding the 2-D omnidirectional WPT theory would make it relatively easy to appreciate the three dimensional one reported in Part II.**

***Index Terms*—Magnetic resonance, omnidirectional wireless power, wireless power transfer.**

I. Introduction

THE wireless power transfer (WPT) system based on magnetic resonance for short- and mid-range power transfer was reported by Nicola Tesla a century ago [1]. With the maturity of power electronics for providing high-frequency power supply and the availability of Litz wire for the coil resonator with a high quality factor in the 1980's, WPT has got the required technologies and attracted a lot of attention. WPT research and developments have been applied to medical implants [2]–[5], inductive power transfer systems [6]–[9], and wireless charging systems for portable equipment such as mobile phones [10]–[15]. While most of the previous works focus on directional WPT, the idea of using orthogonal coils for omnidirectional WPT is addressed in [16], which highlights the point that identical currents in the orthogonal coils will not lead to true omnidirectional WPT. This point is also confirmed with experiments in [17]. Recent advancements in the control principles of true omnidirectional WPT have been reported in [18].

Manuscript received August 20, 2015; revised October 28, 2015 and January 11, 2016; accepted January 20, 2016. Date of publication January 29, 2016; date of current version September 16, 2016. This work was supported by the General Research Fund of the Hong Kong Research Grant Council under Project HKU 17206715. Recommended for publication by Associate Editor M. Duffy.

D. Lin and C. Zhang are with the Department of Electrical and Electronic Engineering, University of Hong Kong, Pokfulam, Hong Kong (e-mail: deyanlin@eee.hku.hk; czhang@eee.hku.hk).

S. Y. R. Hui is with the Department of Electrical and Electronic Engineering, Imperial College London, London SW7 2AZ, U.K., and also with the Department of Electrical and Electronic Engineering, University of Hong Kong, Pokfulam, Hong Kong (e-mail: ronhui@eee.hku.hk).

Color versions of one or more of the figures in this paper are available online at http://ieeexplore.ieee.org.

Digital Object Identifier 10.1109/TPEL.2016.2523500

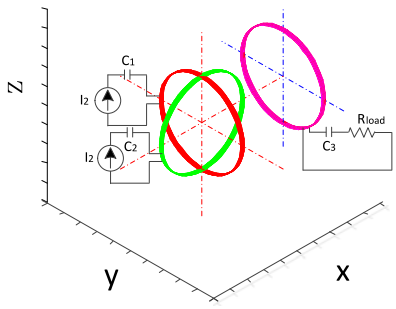

Fig. 1. Two-dimensional omnidirectional WPT system with a loaded receiver coil resonator.

So far, there is still a lack of theoretical understanding of omnidirectional WPT. Parts I and II of this paper aim at providing the theoretical basis on which two-dimensional (2-D) and three-dimensional (3-D) omnidirectional WPT systems can be analyzed so that their characteristics can be identified and explored. In Part-I, a theoretical analysis of 2-D omnidirectional WPT is presented. This paper is an extended version of [22]. It analyzes the relationships of the input power, output power, and energy efficiency for any angular position between the load and the magnetic field vector generated by two orthogonal transmitter coils. It is demonstrated that by using proper current control, "rotating magnetic field vector" can be generated and that the total input power, output power, and energy efficiency of the system follow the Lemniscates of Bernoulli. Under the said operating conditions, the energy efficiency of the whole system should reach maximum point or minimum point just as the sinusoidal-shaped input power reaches its maximum or minimum point along the angular position. Therefore, this phenomenon could be used to locate the positions of the receivers with only a few measurements on the input (transmitter) side. Consequently, wireless power can be directed to the receivers in an energy efficient manner. These features derived from the theory have been practically identified in an experimental setup.

II. Theoretical Analysis of 2-D Omnidirectional WPT

A 2-D WPT system is shown in Fig. 1, in which the first (red) coil and the second (green) coil are two orthogonal transmitter coils, and the third (pink) coil is the receiver coil loaded with a series resonant capacitor and a resistive load $R_{\rm load}$. The use of orthogonal transmitter coils for omnidirectional WPT systems has previously been addressed in [16], [17], and [21]. Orthogonal coils have theoretically no mutual inductance. The nonidentical current control reported in [17] and [21] create a rotating resultant magnetic field vector in 2-D and 3-D

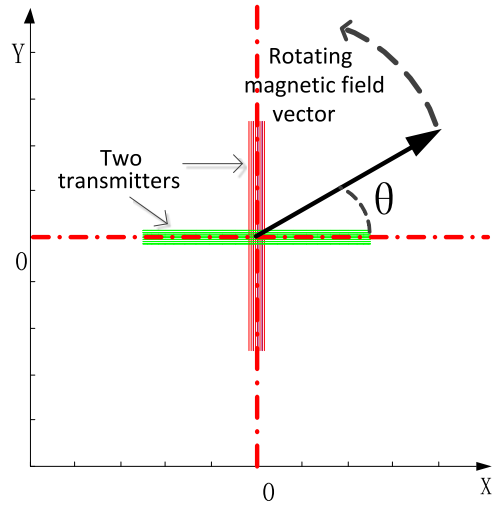

Fig. 2. Schematic diagram of the two orthogonal transmitter coils and a typical rotating magnetic field vector.

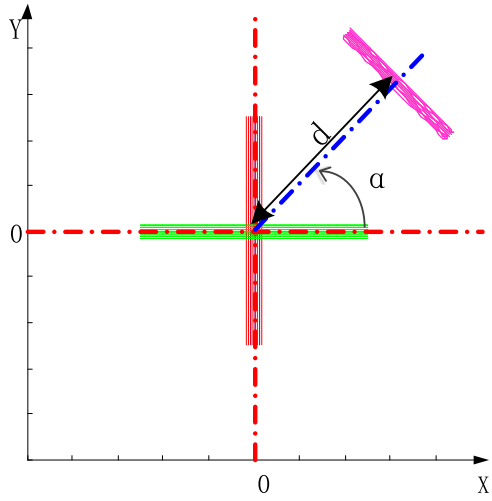

Fig. 3. Geometrical relationship of a loaded receiver coil resonator in a 2-D omnidirectional structure.

omnidirectional manners. It has been pointed out that identical currents in the two orthogonal coils cannot generate the rotating magnetic field vector in a truly omnidirectional manner [16], [17]. The nonidentical current method has been proposed to ensure genuine omnidirectional WPT. For a 2-D WPT system, the two orthogonal transmitter coils are excited with two non-identical ac current sources $\mathbf{I}_1$ and $\mathbf{I}_2$ in order to generate the magnetic field vector. There are different forms of nonidentical currents that can generate the rotating magnetic field vector for omnidirectional WPT. In this analysis, these two current sources have the same frequency and phase, but are different in terms of their amplitude modulation functions. Mathematically

$$\begin{bmatrix} \mathbf{I}_1 \\ \mathbf{I}_2 \end{bmatrix} = \begin{bmatrix} \cos\theta \\ \sin\theta \end{bmatrix} I \tag{1}$$

where $\cos\theta$ and $\sin\theta$ are the amplitude modulation functions of $\mathbf{I}_1$ and $\mathbf{I}_2$, respectively; θ is the physical angle of the resultant magnetic field vector on the 2-D plane as shown in Fig. 2, and I is a sinusoidal time function. The resultant magnetic field vector is the vectorial sum of the two individual magnetic field vectors formed by the two current-excited transmitter coils as shown in Fig. 2, where θ is the angle and $0^\circ \leq \theta < 360^\circ$. Assuming that the receiver can be placed around the transmitters with its plane facing the center of the transmitter coils (i.e., the origin of the coordinates of the transmitter coils) as shown in Fig. 3, then, the receiver will always pick up power; hence, a 2-D omnidirectional WPT system can be formed.

The coupled circuit equation of the three-coil WPT system is given in (2) as shown at the bottom of the page. $\mathbf{U}_1$ and $\mathbf{U}_2$ are the equivalent voltages of the transmitter circuits that provide the current sources $\mathbf{I}_1$ and $\mathbf{I}_2$ for the two transmitter coils. If all the parameters in the matrix in (2) are known (i.e., L_i, R_i, and M_{ij} could be measured or calculated [19], C_i and R_{load} could be measured or identified by evolutionary approach using measured input voltages and currents at the transmitter side [20]), then, $\mathbf{U}_1$, $\mathbf{U}_2$, $\mathbf{I}_3$, the power transmitted from the two transmitters to the receiver, and the overall efficiency of the power transmitting can be calculated.

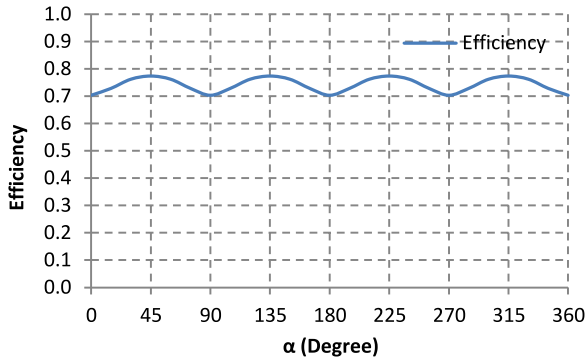

Fig. 4. Energy efficiency of the 2-D WPT system when the receiver-load is placed around the origin of the two transmitter coils (which are excited with another nonidentical current control with the two currents of the same magnitude and a phase difference of 90°). [17], [18].

Fig. 4 shows the simulated energy efficiency results against the angular position for a 2-D omnidirectional WPT system in which the two transmitters are driven by two current sources which have the same magnitude but with a phase difference of 90°. (Note: this is another form of the nonidentical current

$$\begin{bmatrix} \mathbf{U}_1 \\ \mathbf{U}_2 \\ 0 \end{bmatrix} = \begin{bmatrix} R_1 + j\left(\omega L_1 - \frac{1}{\omega C_1}\right) & j\omega M_{12} & j\omega M_{13} \\ j\omega M_{12} & R_2 + j\left(\omega L_2 - \frac{1}{\omega C_2}\right) & j\omega M_{23} \\ j\omega M_{13} & j\omega M_{23} & R_3 + R_{\text{load}} + j\left(\omega L_3 - \frac{1}{\omega C_3}\right) \end{bmatrix} \begin{bmatrix} \mathbf{I}_1 \\ \mathbf{I}_2 \\ \mathbf{I}_3 \end{bmatrix} \tag{2}$$

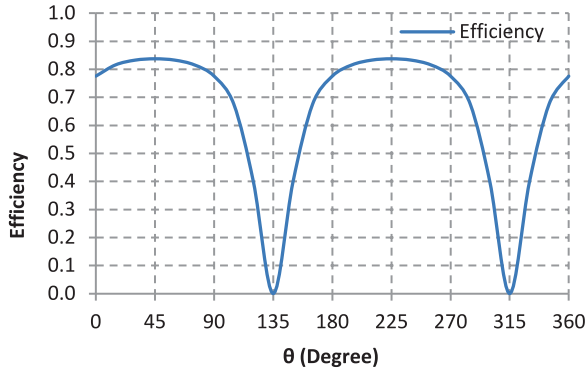

Fig. 5. Efficiency when the magnetic vector is rotating around the origin and the load is placed at 45°.

method used in [17].) The energy efficiency is obtained by placing the load in different angles over 360° in the presence of a rotating magnetic field vector. The parameters used for the simulation are: the two transmitter coil diameters are $d_1 = 0.3$ m and $d_2 = 0.3$ m, the number of turns in the transmitter coils are $T_1 = 11$ and $T_2 = 11$, the self-inductance values of the two transmitters are $L_1 = L_2 = 82.03$ μH, the receiver coil's diameter is $d_3 = 0.3$ m, the number of turns of the receiver coil is $T_3 = 11$, the self-inductance of the receiver coil is $L_3 = 82.03$ μH, the distance between the transmitters' center and the receiver's center is $d = 0.3$ m, $C_1 = C_2 = C_3 = 1$ nF, the transmitter coil resistances are $R_1 = R_2 = 0.9998$ Ω, the receiver coil resistance is $R_3 = 0.9998$ Ω, the load resistance is $R_{\text{load}} = 10$ Ω, the operating frequency $f = 535$ kHz ($\omega = 3.36 * 10^6$ rad/s), and the transmitter coil current magnitude is 0.15 A. The position of the receiver is expressed in polar coordinates: $d \angle \alpha$, where α is the angle as shown in Fig. 3.

This kind of rotating magnetic field will ensure that the load(s) at any direction on the 2-D plane can pick up power [17], [18]. It is the simplest form of a 2-D omnidirectional WPT system, although it is not necessarily the most efficient way to power the load, especially when there is only one load in the plain (because the rotating magnetic field vector will point at a range of angles where there is no load). When there is only one receiver in the WPT system, it is better to direct the magnetic field vector to point directly at the receiver in order to achieve the optimal performance [17], [18]. Fig. 5 shows the energy efficiency of the same setup when the resultant magnetic vector generated by the input current $\mathbf{I}_1$ and $\mathbf{I}_2$ as shown in (1) rotating around the origin along with θ increasing, and the receiver's position is placed at $\alpha = 45°$ as shown in Fig. 3, where $d = 0.3$ m. The maximum efficiency in Fig. 5 is much higher than the maximum efficiency which is shown in Fig. 4. The calculations of the input power and output power as well as the efficiency will be shown below.

Comparison of Figs. 4 and 5 indicates that the optimal strategy is to scan the magnetic field vector to detect the load positions (omnidirectional load detection) and then to focus the power toward the load directions (directional power flow control) as explained in [21].

Since the two transmitter coils are orthogonal to each other, $M_{12} = 0$. Equation (2) could be rewritten as (3) shown at the bottom of the page.

After substituting (1) into (3)

$$\begin{bmatrix} \mathbf{U}_1 \\ \mathbf{U}_2 \\ 0 \end{bmatrix} = \begin{bmatrix} R_1 + jX_1 & 0 & j\omega M_{13} \\ 0 & R_2 + jX_2 & j\omega M_{23} \\ j\omega M_{13} & j\omega M_{23} & R_3 + R_{\text{load}} + jX_3 \end{bmatrix} \times \begin{bmatrix} I\cos\theta \\ I\sin\theta \\ \mathbf{I}_3 \end{bmatrix} \tag{4}$$

where

$$X_1 = \left(\omega L_1 - \frac{1}{\omega C_1}\right), X_2 = \left(\omega L_2 - \frac{1}{\omega C_2}\right), X_3 = \left(\omega L_3 - \frac{1}{\omega C_3}\right).$$

A. Load Current Calculation

From (4), it can be shown that

$$j\omega M_{13} I\cos\theta + j\omega M_{23} I\sin\theta + (R_3 + R_{\text{load}} + jX_3)\mathbf{I}_3 = 0 \tag{5}$$

Rearranging (5) leads to

$$\mathbf{I}_3 = -\frac{j\omega I}{R_3 + R_{\text{load}} + jX_3}(M_{13}\cos\theta + M_{23}\sin\theta) \tag{6}$$

or

$$\mathbf{I}_3 = -\frac{j\omega I\sqrt{M_{13}^2 + M_{23}^2}}{R_3 + R_{\text{load}} + jX_3}\sin\left(a\tan\frac{M_{13}}{M_{23}} + \theta\right) \tag{7}$$

where the amplitude of I_3 is

$$I_3 = \frac{I\omega\sqrt{M_{13}^2 + M_{23}^2}}{\sqrt{(R_3 + R_{\text{load}})^2 + X_3^2}}\left|\sin\left(a\tan\frac{M_{13}}{M_{23}} + \theta\right)\right| \tag{8}$$

Equation (8) provides the load current information.

B. Output Power Calculation

1) P_{load}: Load power

The load power can be expressed as

$$P_{\text{load}} = I_3^2 R_{\text{load}} = I^2\left(\frac{R_{\text{load}}\omega^2(M_{13}^2 + M_{23}^2)}{(R_3 + R_{\text{load}})^2 + X_3^2} \times \sin^2\left(a\tan\frac{M_{13}}{M_{23}} + \theta\right)\right) \tag{9}$$

$$\begin{bmatrix} \mathbf{U}_1 \\ \mathbf{U}_2 \\ 0 \end{bmatrix} = \begin{bmatrix} R_1 + j\left(\omega L_1 - \frac{1}{\omega C_1}\right) & 0 & j\omega M_{13} \\ 0 & R_2 + j\left(\omega L_2 - \frac{1}{\omega C_2}\right) & j\omega M_{23} \\ j\omega M_{13} & j\omega M_{23} & R_3 + R_{\text{load}} + j\left(\omega L_3 - \frac{1}{\omega C_3}\right) \end{bmatrix} \begin{bmatrix} \mathbf{I}_1 \\ \mathbf{I}_2 \\ \mathbf{I}_3 \end{bmatrix} \tag{3}$$

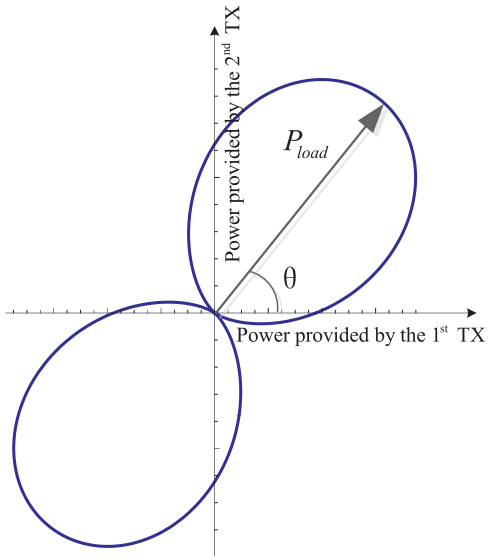

Fig. 6. Load power plot (in the form of a Lemniscate of Bernoulli).

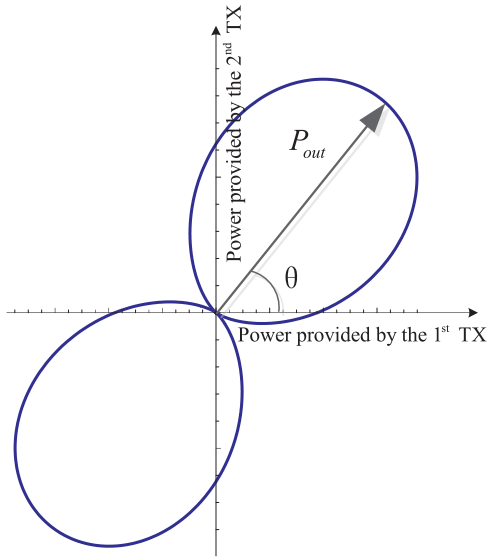

Fig. 7. Plot of the power picked up by the receiver (in the form of the Lemniscate of Bernoulli).

Equation (9) can be simplified as (10), which is in the form of a Lemniscate of Bernoulli as shown in Fig. 6. The load power is represented in Fig. 6 as a vector with a magnitude and a direction. The positive direction is defined by the right-hand rule of the current flowing in a coil

$$P_{\text{load}} = K_{2-D} I^2 R_{\text{load}} \sin^2(\gamma_{2-D} + \theta) \tag{10}$$

where

$$K_{2-D} = \frac{\omega^2 (M_{13}^2 + M_{23}^2)}{(R_3 + R_{\text{load}})^2 + X_3^2} \tag{11}$$

$$\gamma_{2-D} = a\tan\frac{M_{13}}{M_{23}} \tag{12}$$

When $\sin^2(\gamma_{2-D} + \theta) = 1$, i.e., $\gamma_{2-D} + \theta = \frac{\pi}{2}$ or $\frac{3\pi}{2}$, P_{load} reaches its maximum value

$$P_{\text{load\_max}} = K_{2-D} I^2 R_{\text{load}} \tag{13}$$

When $\sin^2(\gamma_{2-D} + \theta) = 0$, i.e.,$\gamma_{2-D} + \theta = 0$ or π, P_{load} reaches its minimum value

$$P_{\text{load\_min}} = 0 \tag{14}$$

2) P_{out}: Power Picked Up by the Receiver

The equation of the power transferred to the receiver is

$$\begin{aligned} P_{\text{out}} &= I_3^2 R_3 + I_3^2 R_{\text{load}} \\ &= K_{2-D} I^2 (R_3 + R_{\text{load}}) \sin^2(\gamma_{2-D} + \theta) \end{aligned} \tag{15}$$

It can be seen that the power received is also a Lemniscate of Bernoulli, as shown in Fig. 7. Again, the output power is represented as a vector with a magnitude and a direction.

When $\sin^2(\gamma_{2-D} + \theta) = 1$, i.e.,$\gamma_{2-D} + \theta = \frac{\pi}{2}$ or $\frac{3\pi}{2}$, P_{out} reaches its maximum value

$$P_{\text{out\_max}} = K_{2-D} I^2 (R_3 + R_{\text{load}}) \tag{16}$$

When $\sin^2(\gamma_{2-D} + \theta) = 0$, i.e.,$\gamma_{2-D} + \theta = 0$ or π, P_{out} reaches its minimum value

$$P_{\text{out\_min}} = 0 \tag{17}$$

C. Input Power Calculation

The power losses in the two transmitter coils and the receiver coil are

$$P_{\text{loss1}} = I_1^2 R_1 = I^2 R_1 \cos^2\theta \tag{18}$$

$$P_{\text{loss2}} = I_2^2 R_2 = I^2 R_2 \sin^2\theta \tag{19}$$

$$P_{\text{loss3}} = I_3^2 R_3 \tag{20}$$

The load power is

$$P_{\text{load}} = I_3^2 R_{\text{load}} \tag{21}$$

The total input power is therefore

$$P_{\text{in}} = P_{\text{loss1}} + P_{\text{loss2}} + P_{\text{loss3}} + P_{\text{load}} \tag{22}$$

Substituting (8) and (18)–(21) into (22) results as follows:

$$\begin{aligned} P_{\text{in}} = I^2 \Bigg(&(R_1 \cos^2\theta + R_2 \sin^2\theta) + \frac{(R_3 + R_{\text{load}})\omega^2 (M_{13}^2 + M_{23}^2)}{(R_3 + R_{\text{load}})^2 + X_3^2} \\ &\times \sin^2\left(a\tan\frac{M_{13}}{M_{23}} + \theta\right)\Bigg) \end{aligned} \tag{23}$$

Equation (23) can be reexpressed as follows:

$$\begin{aligned} P_{\text{in}} = {} & I^2 (R_1 + (R_2 - R_1)\sin^2\theta \\ & + K_{2-D}(R_3 + R_{\text{load}})\sin^2(\gamma_{2-D} + \theta)) \end{aligned} \tag{24}$$

If $R_1 = R_2 = R$, then

$$P_{\text{in}} = I^2 R + K_{2-D} I^2 (R_3 + R_{\text{load}}) \sin^2(\gamma_{2-D} + \theta) \tag{25}$$

It is a deformed Lemniscate of Bernoulli in which the deformation occurs near the origin of Fig. 8. It should be noted

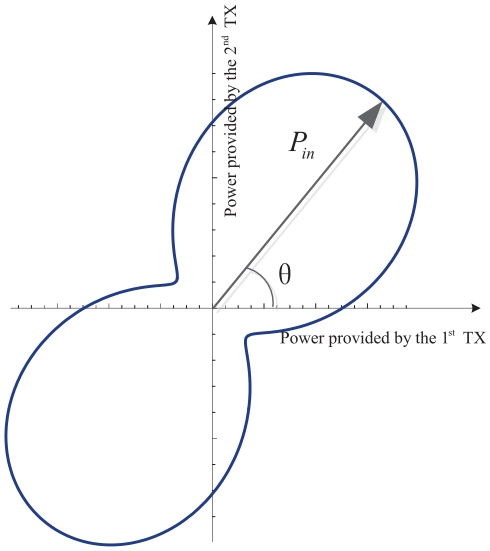

Fig. 8. Plot of the input power (in the form of a deformed Lemniscate of Bernoulli).

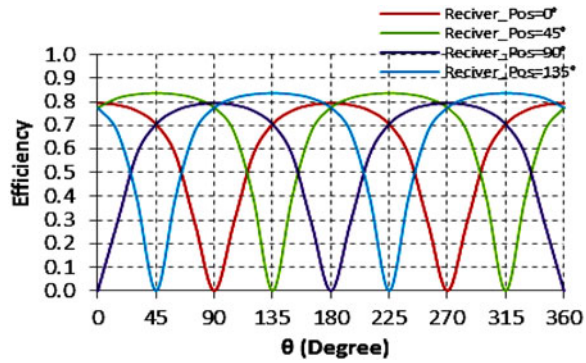

Fig. 9. Energy Efficiency plots when the receiver is placed at different angle α and the receiver's center $d = 0.3$ m, and the two transmitter coils producing a rotating magnetic field.

that the difference between (15) and (25) is the term I^2R in the right-hand side of (25). This extra I^2R term is the reason for the deformation of the Lemiscate near the origin.

When $\sin^2(\gamma_{2-D}+\theta)=1$, i.e.,$\gamma_{2-D}+\theta=\frac{\pi}{2}$ or $\frac{3\pi}{2}$, P_{in} reaches its maximum value as

$$P_{\text{in\_max}} = I^2(R + K_{2-D}(R_3 + R_{\text{load}})) \tag{26}$$

When $\sin^2(\gamma_{2-D}+\theta)=0$, i.e.,$\gamma_{2-D}+\theta=0$ or π, P_{in} reaches its minimum value as

$$P_{\text{in\_min}} = I^2R \tag{27}$$

D. Efficiency Calculation

The energy efficiency is mathematically expressed as

$$\begin{aligned}\eta = \frac{P_{\text{load}}}{P_{\text{in}}} &= \frac{K_{2-D}I^2R_{\text{load}}\sin^2(\gamma_{2-D}+\theta)}{I^2R + K_{2-D}I^2(R_3+R_{\text{load}})\sin^2(\gamma_{2-D}+\theta)} \\ &= \frac{K_{2-D}R_{\text{load}}\sin^2(\gamma_{2-D}+\theta)}{R + K_{2-D}(R_3+R_{\text{load}})\sin^2(\gamma_{2-D}+\theta)} \\ &= \frac{R_{\text{load}}}{\frac{R}{K_{2-D}\sin^2(\gamma_{2-D}+\theta)} + (R_3+R_{\text{load}})}\end{aligned} \tag{28}$$

When $\sin^2(\gamma_{2-D}+\theta)=1$, i.e.,$\gamma_{2-D}+\theta=\frac{\pi}{2}$ or $\frac{3\pi}{2}$, η reaches its maximum value, just as P_{in} does. Thus

$$\eta_{\max} = \frac{R_{\text{load}}}{\frac{R}{K_{2-D}} + (R_3+R_{\text{load}})} \tag{29}$$

When $\sin^2(\gamma_{2-D}+\theta)=0$, i.e., $\gamma_{2-D}+\theta=0$ or π, η reaches its minimum value

$$\eta_{\min} = 0 \tag{30}$$

Figs. 6–8 could also be represented in the Cartesian coordinate system. As an example, Fig. 9 shows the simulated results of the energy efficiency for the 2-D omnidirectional WPT system in the Cartesian coordinate system with fixed transmitters–receiver distance $d = 0.3$ m and angular positions of 0°, 45°, 90°, and 135°.

E. Physical Implications of the Input Power in the Form of the Lemniscate of Bernoulli

Since input power can be measured on the transmitter side, its Lemniscate of Bernoulli offers important information in relation to the direction of the load, load resistance, and the load power. Considering (11) and (12) in relation to (25), the input power equation in (25) consists of five known parameters (ω, I, R, R_3, and X_3) and three unknown variables (M_{13}, M_{23}, and R_{load}). The three unknowns can be theoretically calculated by measuring the input power at three different angles $\theta_1, \theta_2, \theta_3$

$$\begin{cases} P_{\text{in1}} = I^2R + K_{2-D}I^2(R_3+R_{\text{load}})\sin^2(\gamma_{2-D}+\theta_1) \\ P_{\text{in2}} = I^2R + K_{2-D}I^2(R_3+R_{\text{load}})\sin^2(\gamma_{2-D}+\theta_2) \\ P_{\text{in3}} = I^2R + K_{2-D}I^2(R_3+R_{\text{load}})\sin^2(\gamma_{2-D}+\theta_3) \end{cases} \tag{31}$$

With the load resistance R_{load} determined, the angular location of the load can also be found. To illustrate this idea, first rewrite (25) as

$$P_{\text{in}} = I^2R + I^2A_{2-D}\sin^2(\gamma_{2-D}+\theta) \tag{32}$$

where A_{2-D} is a constant and $A_{2-D} = K_{2-D}(R_3+R_{\text{load}})$. The total input power curve versus θ is a sinusoidal relationship with a known offset I^2R. One can use only two measurements of the total input power at different current vector angles (θ_1, θ_2) to calculate A_{2-D} and γ_{2-D}, then predict the angle θ_m, at which the maximum input power will be achieved. From (10), (16), and (29), it can be observed that the load power, the output power (power picked up by the receiving coil), and the energy efficiency will reach their maximum at the angle θ_m, as the input power does. Therefore, the angle of the load can be determined theoretically. In practice, the locations of the loads can also be determined by the power vectors reported in [21].

In the above analysis, it is assumed that the center of the receiver coil faces the transmitter system. If the plane of the

receiver coil is parallel to the 2-D plane of the 2-D WPT system and passes the center of the transmitter coils (i.e., the origin of the coordinates of the transmitter coils), the receiver will not receive any power theoretically. This is an inherent limitation of a 2-D WPT if the receiver consists of only one planar receiver coil. To overcome this problem, two orthogonal coils can be used to form the receiver coil as explained in [16].

F. Electromagnetic Position

The angle of the magnetic field vector θ at which the maximum power flows may not be identical with the actual physical angle α of the receiver coil. The magnetic vector analysis assumes that the magnetic flux generated by a coil flows indefinitely along one direction in a straight line. In practice, the magnetic flux will deviate from a straight path so that the lines of flux will form closed return paths in the surrounding space of the transmitter–coil system. The effects of the spatial distribution of the magnetic field can be accounted for in the mutual inductance calculation of the system model [19]. Based on the mathematical model of the 2-D WPT system (including the effects of the spatial distribution), the predicted angular positions (at which the maximum power flows) are plotted against the physical angular positions of the receiver coil (with the receiver coil plane facing the central of the 2-D transmitter–coil system) in Fig. 10. It can be seen that there is deviation between the angular angle of the maximum power flow and the physical angular position of the receiver coil, except at 45°, 90°, 135°, and 180°. At these four angles, the symmetry of the magnetic flux patterns generated by the two transmitter coil currents leads to the cancellation of the effects caused by the spatial distribution of the magnetic fields. Despite the fact that the maximum power flow angle may not be exactly the same as the physical angle, a general control technique for omnidirectional WPT systems has been developed [21]. This method involves a scanning process in which the magnetic vector is generated to point at discrete angles in a uniform manner (in a circular space for a 2-D system and a spherical space for a 3-D system). By recording the power associated with each vector, the direction(s) at which the power flow is required can be determined in a practical system. Directional power flow can then be used to focus WPT toward the targeted load area(s) in an energy-efficiency manner.

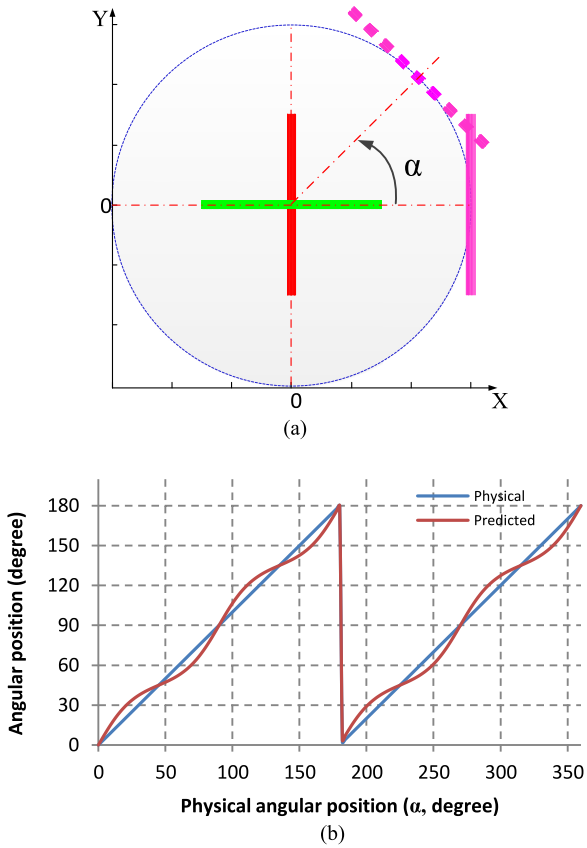

Fig. 10. (a) Relative location of the receiver coil with the two orthogonal transmitter coils (with the receiver coil facing the central of the transmitter coil system and moved along the dashed circle). (b) Predicted angle of maximum power flow against the physical angle of the receiver coil [corresponding to various positions in Fig. 10(a)].

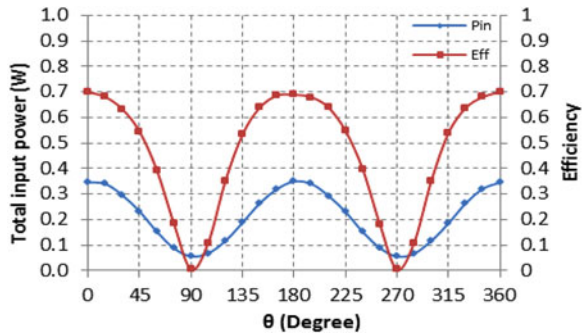

Fig. 11. Total input power and efficiency when the receiver fixed at the position of 0° and the two transmitters producing a circular rotating magnetic field.

III. Experimental Verifications

The 2-D omnidirectional WPT system shown in Fig. 3 has been setup. The receiver coil is placed at the angular positions at 0°, 45°, 90°, and 135° for practical evaluation. The experimental results are included in Figs. 11 to 18 with the same parameters for simulation in Section II. In these figures, Figs. 11, 13, 15, and 17 are the measured total input power and efficiency against the magnetic vector angle θ for the receiver position angles of 0°, 45°, 90°, and 135°, respectively. The corresponding measurements of the Lemniscate of Bernoulli plots for the total input power for these four angular positions of the receiver coil are shown in Figs. 12, 14, 16, and 18, respectively. In these four figures, the power is represented in the vector form. The positive value of the input power means that the coil provides power to the receiver coil at its "positive" direction, while the negative value of the input power means that the coil provides power to the receiver coil at its "negative" direction. The direction of the transmitter coil is defined by the right-hand rule according to the current direction reference of the coil. It is noted that these Lemniscates of Bernoulli confirm that the power flow is directed to the directions of the loaded receiver coil positions.

The theoretical results based on the 2-D WPT theory are compared with the experimental ones in Figs. 19 and 20. Fig. 19(a)

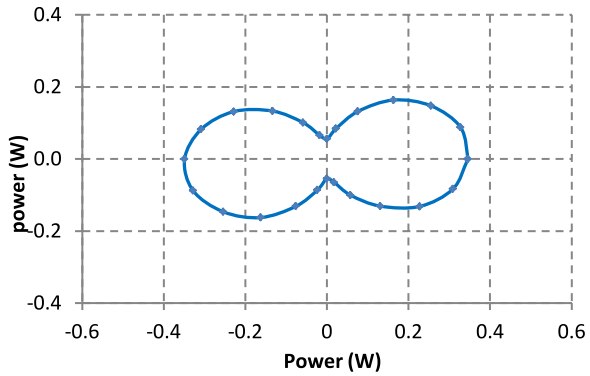

Fig. 12. Measured Lemniscate of Bernoulli curves for the total input power at the angle receiver position = 0°.

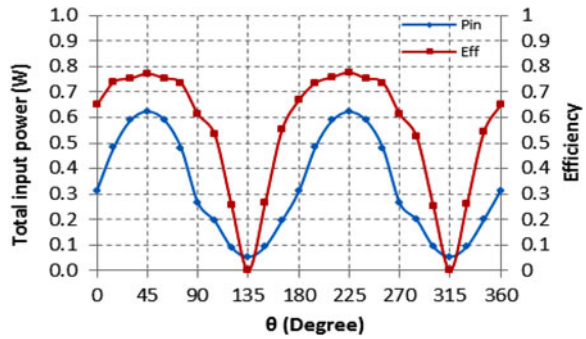

Fig. 13. Total input power and efficiency when the receiver's angle α is fixed at the position of 45° and the two transmitters producing a circular rotating magnetic field.

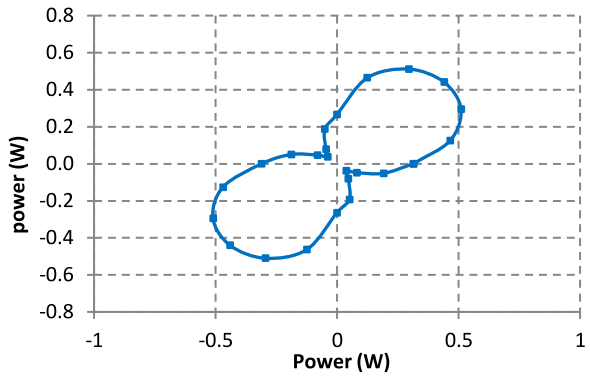

Fig. 14. Measured Lemniscate of Bernoulli curves for total input power at the angle receiver position = 45°.

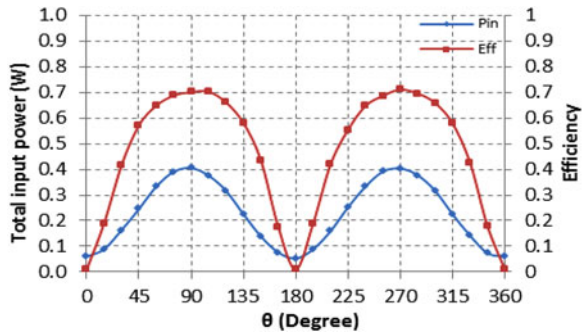

Fig. 15. Total input power and efficiency when the receiver's angle α is fixed at the position of 90° and the two transmitters producing a circular rotating magnetic field.

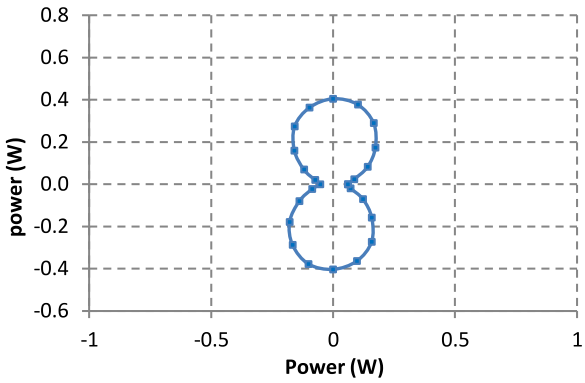

Fig. 16. Measured Lemniscate of Bernoulli curves for total input power at the angle receiver position = 90°.

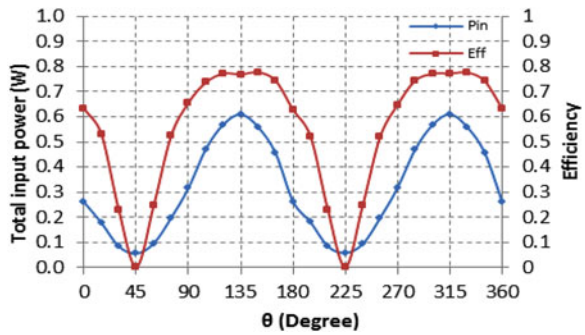

Fig. 17. Total input power and efficiency when the receiver's angle α is fixed at the position of 135° and the two transmitters producing a circular rotating magnetic field.

shows the experimental input power over 360° on the 2-D plane with the receiver placed at four different angular positions. The corresponding theoretical results are included in Fig. 19(b). It can be seen that the theoretical and experimental have good agreements. The slight differences are believed to be due to the minor differences between the practical system parameters and the theoretical ones (such as the capacitances C_1, C_2, and C_3, the resistances R_1, R_2, and R_3, and the calculated self-inductances of the three coils or mutual inductances between the coils). Fig. 20(a) shows the experimental results of the energy efficiency over 360° on the 2-D plane with the receiver placed at four different angular positions. The corresponding theoretical results are shown in Fig. 20(b). Again, they exhibit good agreements.

In each comparison of the total input power and efficiency, it can be seen that the total input power is sinusoidal over the 360°, while the maximum power points coincide with the maximum energy efficiency points.

These comparisons in Figs. 19 and 20 confirm that the analysis of the input power and energy efficiency based on the

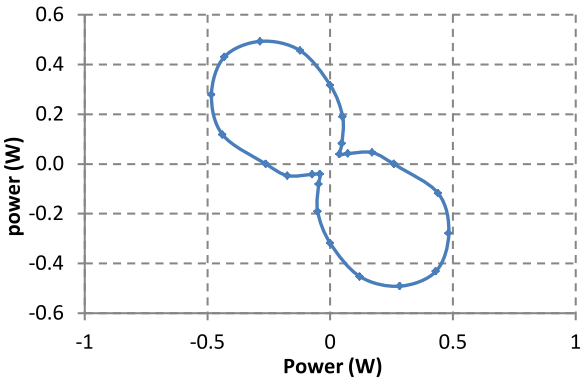

Fig. 18. Measured Lemniscate of Bernoulli curves for total input power at the angle receiver position = 135°.

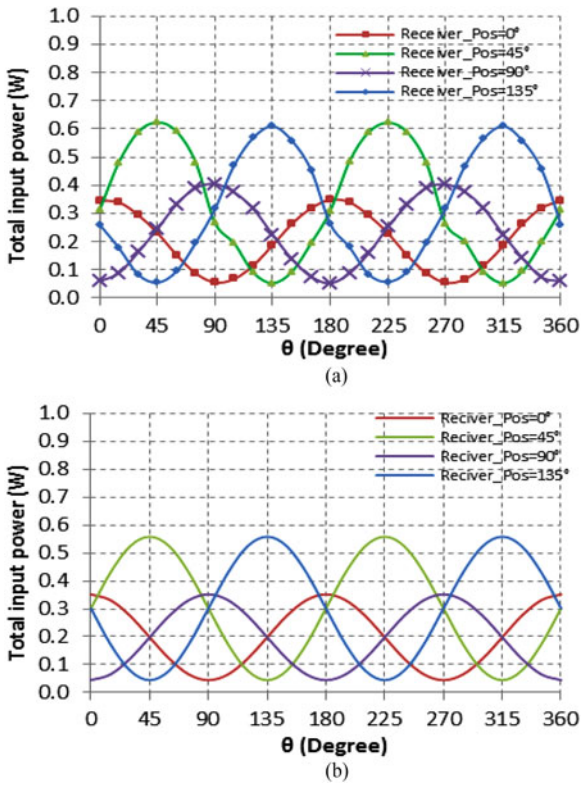

Fig. 19. Experimental and simulated total input power when the receiver's angle α is fixed at the position of 0°, 45°, 90°, and 135° and the two transmitters producing a circular rotating magnetic field. (a) Experimental results. (b) Simulated results.

2-D omnidirectional WPT theory is correct. Obviously, using the measured input power to indicate the angular position of the load and to predict the maximum efficiency direction is feasible.

IV. Conclusion

This paper provides a theoretical analysis on the relationships between the total input power, load power, output power, and efficiency for 2-D omnidirectional WPT systems. It is proved that, the total input power of a 2-D omnidirectional WPT system is a sinusoidal function of the angle of the rotating current vector

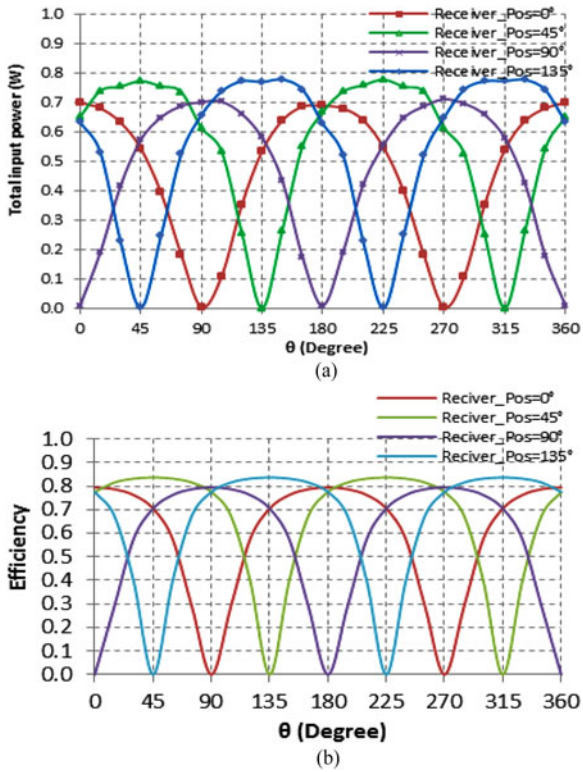

Fig. 20. Experimental and simulated efficiency when the receiver's angle α is fixed at the position of 0°, 45°, 90°, and 135° and the two transmitters producing a circular rotating magnetic field. (a) Experimental results. (b) Simulated results.

on the 2-D plane. The functions of the total input power, load power, output power, and energy efficiency are Lemniscates of Bernoulli. The profile of the energy efficiency of the system approximately follows that of the total input power. According to our analysis, the maximum energy transfer and maximum efficiency direction is independent of the load resistance, and also independent of the operating frequency. Thus, one can predict the load position by making only a few measurements. In the best case, two measurements are sufficient to locate the load direction. Once the exact direction of the load in an omnidirectional WPT system is obtained, one can predict the performance of the system and choose the optimized driving strategy such as maximum power transfer or maximum efficiency. It should be noted that all measurements can be obtained on the transmitter side. This analysis method can be extended to 3-D omnidirectional WPT systems.

References

[1] N. Tesla, "Apparatus for transmitting electrical energy," U.S. Patent 1 119 732, Dec. 1, 1914.
[2] J. Schuder, H. Stephenson, and J. Townsend, "High-level electromagnetic energy transfer through a closed chest wall," *Inst. Radio Eng. Int. Conv. Rec.*, vol. 9, pp. 119–126, 1961.
[3] W. Ko, S. Liang, and C. F. Fung, "Design of radio-frequency powered coils for implant instruments," *Med. Biol. Eng. Comput.*, vol. 15, pp. 634–640, Nov. 1, 1977.
[4] E. S. Hochmair, "System optimization for improved accuracy in transcutaneous signal and power transmission," *IEEE Trans. Biomed. Eng.*, vol. BME-31, no. 2, pp. 177–186, Feb. 1984.
[5] N. Kyungmin, J. Heedon, M. Hyunggun, and F. Bien, "Tracking optimal efficiency of magnetic resonance wireless power transfer system

for biomedical capsule endoscopy," *IEEE Trans. Microw. Theory Techn.*, vol. 63, no. 1, pp. 295–304, Nov. 2014.
[6] J. T. Boys, G. A. Covic, and A. W. Green, "Stability and control of inductively coupled power transfer systems," *Proc. IEE-Elect. Power Appl.*, vol. 147, pp. 37–43, 2000.
[7] J. T. Boys, A. P. Hu, and G. A. Covic, "Critical Q analysis of a current-fed resonant converter for ICPT applications," *Electron. Lett.*, vol. 36, pp. 1440–1442, 2000.
[8] G. A. J. Elliott, G. A. Covic, D. Kacprzak, and J. T. Boys, "A new concept: Asymmetrical pick-ups for inductively coupled power transfer monorail systems," *IEEE Trans. Magn.*, vol. 42, no. 10, pp. 3389–3391, Oct. 2006.
[9] M. L. G. Kissin, J. T. Boys, and G. A. Covic, "Interphase mutual inductance in polyphase inductive power transfer systems," *IEEE Trans. Ind. Electron.*, vol. 56, no. 7, pp. 2393–2400, Apr. 2009.
[10] C.-G. Kim, D.-H. Seo, J.-S. You, J.-H. Park, and B. H. Cho, "Design of a contactless battery charger for cellular phone," *IEEE Trans. Ind. Electron.*, vol. 48, no. 6, pp. 1238–1247, Dec. 2001.
[11] J. Yungtaek and M. M. Jovanovic, "A contactless electrical energy transmission system for portable-telephone battery chargers," *IEEE Trans. Ind. Electron.*, vol. 50, no. 3, pp. 520–527, Jun. 2003.
[12] C. Byungcho, N. Jaehyun, C. Honnyong, A. Taeyoung, and B. Choi, "Design and implementation of low-profile contactless battery charger using planar printed circuit board windings as energy transfer device," *IEEE Trans. Ind. Electron.*, vol. 51, no. 1, pp. 140–147, Feb. 2004.
[13] S. Y. R. Hui and W. W. C. Ho, "A new generation of universal contactless battery charging platform for portable consumer electronic equipment," *IEEE Trans. Power Electron.*, vol. 20, no. 3, pp. 620–627, May 2005.
[14] X. Liu and S. Y. R. Hui, "Simulation study and experimental verification of a universal contactless battery charging platform with localized charging features," *IEEE Trans. Power Electron.*, vol. 22, no. 6, pp. 2202–2210, Nov. 2007.
[15] S. Y. R. Hui, "Planar inductive battery charging system," U.S. Patent 7 576 514, Aug. 18, 2009.
[16] K. O'Brien, "Inductively coupled radio frequency power transmission system for wireless systems," Ph.D. dissertation, School of Engineering Sciences, Faculty of Electrical and Computer Engineering, Technische Universitat Dresden, Dresden, Germany, 2007, pp. 47–62.
[17] W. M. Ng, C. Zhang, D. Lin, and S. Y. R. Hui, "Two- and three-dimensional omnidirectional wireless power transfer," *IEEE Trans. Power Electron.*, vol. 29, no. 9, pp. 4470–4474, Jan. 2014.
[18] C. Zhang, D. Lin, and S. Y. R. Hui, "Systems and methods for load position detection and power control of omni-directional wireless power transfer," PCT Patent Appl. PCT(CN2015(071543, Jan. 26, 2015.
[19] S. Babic and C. Akyel, "Improvement in calculation of the self- and mutual inductance of thin-wall solenoids and disk coils," *IEEE Trans. Magn.*, vol. 36, no. 4, pp. 1970–1975, Jul. 2000.
[20] D. Lin, J. Yin, and S. Y. Hui, "Parameter identification of wireless power transfer systems using input voltage and current," in *Proc. IEEE Energy Convers. Congr. Expo.*, 2014, pp. 832–836.
[21] C. Zhang, D. Lin, and S. Y. R. Hui, "Basic control principles of omnidirectional wireless power transfer," *IEEE Trans. Power Electron.*, vol. 31, no. 7, pp. 5215–5227, Sep. 2015.
[22] D. Lin, C. Zhang, and S. Y. R. Hui, "Power and energy of 2-D omnidirectional wireless power transfer systems," in *Proc. IEEE Energy Convers. Congr. Expo.*, Montreal, OC, Canada, Oct. 2015, pp. 4951–4958.

Deyan Lin (M'09) was born in China, in 1972. He received the B.Sc. and M.A.Sc. degrees from the Huazhong University of Science and Technology, Wuhan, China, in 1995 and 2004, respectively, and the Ph.D. degree from the City University of Hong Kong, Kowloon, Hong Kong, in 2012.

He is currently a Postdoctoral Fellow with the Department of Electrical and Electronic Engineering, University of Hong Kong, Pokfulam, Hong Kong.

From 1995 to 1999, he was a Teaching Assistant with the Electrical Engineering Department, Jianghan University, Wuhan, where he became a Lecturer later. From 2008 to 2009, he was a Senior Research Assistant with the City University of Hong Kong. His current research interests include wireless power transfer, memristors, and modeling, control, simulation of gas-discharge lamps.

Cheng Zhang (S'13) was born in China, in 1990. He received the B.Eng. degree (first class Hons.) in electronic and communication engineering from the City University of Hong Kong, Kowloon, Hong Kong, in 2012. He is currently working toward the Ph.D. degree in the Department of Electrical and Electronic Engineering, University of Hong Kong, Pokfulam, Hong Kong.

His current research interests include designs and optimizations for wireless power transfer applications.

S. Y. Ron Hui (M'87–SM'94–F'03) received the B.Sc. (Hons.) in engineering from the University of Birmingham, Birmingham, U.K., in 1984, and the D.I.C. and Ph.D. degree from the Imperial College London, London, U.K., in 1987.

He currently holds the Philip Wong Wilson Wong Chair Professorship at the University of Hong Kong, Pokfulam, Hong Kong, and a part-time Chair Professorship at the Imperial College London. He has published more than 300 technical papers, including more than 200 refereed journal publications. More than 60 of his patents have been adopted by industry. He is an Associate Editor of the IEEE TRANSACTIONS ON POWER ELECTRONICS and IEEE TRANSACTIONS ON INDUSTRIAL ELECTRONICS, and an Editor of the IEEE JOURNAL OF EMERGING AND SELECTED TOPICS IN POWER ELECTRONICS. His inventions on wireless charging platform technology underpin key dimensions of Qi, the world's first wireless power standard, with freedom of positioning and localized charging features for wireless charging of consumer electronics.

Dr. Hui received the IEEE Rudolf Chope R&D Award from the IEEE Industrial Electronics Society and the IET Achievement Medal (The Crompton Medal), in Nov. 2010, and the 2015 IEEE William E. Newell Power Electronics Award. He is a Fellow of the Australian Academy of Technology & Engineering.